Hydromagnetic Slip Flow of Blood through Porous Medium with Time Dependent Permeability, Pulsatile Pressure and Body Acceleration

Lukendra Kakati[1], Dhruba Prasad Barua[2], Nazibuddin Ahmed[3] and Karabi Dutta Choudhury[4]

[1] Department of Mathematics, Lanka Mahavidyalaya, Lanka, Nagaon-782446, Assam, India

[2, 3] Department of Mathematics, Gauhati University, Guwahati-781014, Assam, India

[4] Department of Mathematics, Assam University, Silchar- 788011, Assam, India

Abstract

The aim of this paper is to investigate the flow of blood through a porous medium with time dependent permeability, in an inclined artery having mild stenosis, in the presence of pulsatile pressure gradient. Here the blood flow is considered to be of Newtonian nature and we impose an azimuthal uniform magnetic field. The fluid flow takes place under body acceleration and we assume the existence of a slip velocity at the stenosed section of the arterial wall. By employing multi-parameter perturbation procedure, we derive solutions for the flow field and wall shear stress and their behaviors are analyzed under the influence of various relevant parameters concerning the magnetic field, slip velocity, porosity, inclination, pulsatile pressure and the periodic body acceleration. The results are displayed pictorially and construed. The results reveal that the azimuthal magnetic field, slip velocity, inclination, pulsatile pressure, periodic body acceleration and the time-dependent permeability of the porous medium play significant roles on the velocity field, and the wall shear stress. For instance, the imposition of the magnetic field causes a decline in the axial velocity of blood and the wall shear stress. On the other hand, a growth in the porosity of the medium leads to a rise in the axial blood velocity as well as the wall shear stress.

1 Introduction

The studies related to blood flow through stenosed arteries have garnered wide interest in the field of Bio-Medical research. Stenosis or atherosclerosis may be defined as the formation of some constriction in the inner arterial wall owing to the deposition of lipoproteins and fatty acids (atherosclerotic plaques) in the lumen of the artery. Such constrictions lead to considerable change in the flow of blood, the pressure distribution and the wall shear stress, thereby impeding the normal circulatory processes and consequently leading to cardiovascular diseases. Even for mild atherosclerosis, the velocity gradient in the stenosed wall is steep owing to the increased core velocity. This results in comparatively large shear stress on the arterial wall. Mathematical models of blood flow through arteries under diverse physiological situations were presented by several authors like Fung [1], McDonald [2], Zamir [3] and David et al. [4]. Theoretical and experimental investigations concerning flow of blood through stenosed arteries were presented by Young [5], Liu et al. [6], Yao and Li [7] and Mekheimer and El-Kot [8]. The human body may be subjected to body accelerations (vibrations) under certain situations such as riding a heavy vehicle or flying in a helicopter. This may cause health problems like vascular disorders and increased pulse rate. Studies related to blood flow under the influence of body acceleration were carried out by several research workers such as Sud and Sekhon [9] and El-Shahed [10]. The Pulsatile nature of blood flow in arteries may be attributed to the heart pulse pressure gradient. Studies in pulsatile blood flow were carried out by researchers like [10] and Elshehawey et al. [11]. The possibility of velocity slip at the blood vessel wall was investigated theoretically by Brunn [12] and Jones [13] and experimentally by Bennet [14] and Bugliarello and Hayden [15]. The methods to detect and

determine slip experimentally at the blood vessel wall have been indicated by Astarita et al. [16] and Cheng [17] respectively. It was first Kolin [18] and later Korchevskii and Marochnik [19] who suggested the scope of electromagnetic fields in Bio-Medical studies. Barnothy [20] indicated that for biological systems, the heart rate decreases under the influence of an external magnetic field. In certain pathological circumstances, the distribution of fatty cholesterol and artery-clogging blood clots in the lumen of the coronary artery may be regarded as equivalent to a fictitious porous medium. Xu et al. [21] assumed the blood clot as a porous medium to investigate the transport characteristics of blood flow in the extension of multi-scale model by incorporating a detailed sub model of surface-mediated control of blood coagulation (Xu et al. [22, 23]). In general, blood is a non-Newtonian fluid. However, it has been established that human blood exhibits Newtonian behavior at all rates of shear for hematocrits up to about 12% [24]. Further, in case of relatively larger blood vessels it is sensible to assume that blood has a constant viscosity, since the diameters of such vessels are large compared with the individual cell diameters and because shear rates are quite high for viscosity to be independent of them. Consequently, for such vessels the non-Newtonian character becomes unimportant and blood may be regarded as a Newtonian fluid.

In view of the aforementioned facts, we may cite the works done by Elshehawey et al. [11], Nagarani and Sarojamma [25], Shehawey and EL Sebaei [26], Tzirtzilakis [27], etc.

The aim of the present study is to investigate theoretically the nature of a pulsatile blood flow through a mildly stenosed artery under the combined influence of an azimuthal uniform magnetic field, slip velocity, body acceleration and time dependent permeability, when the artery is inclined to the vertical. The investigation is carried out by treating blood flow as Newtonian. The solutions have been obtained in terms of Bessel function, using multi-parameter perturbation technique.

2 The formulation of the Problem

For this problem, we take an axially symmetric, laminar, one-dimensional and fully developed blood flow through an inclined and catheterized circular artery, in the presence of a time-dependent pressure gradient, body acceleration and an azimuthally applied magnetic field of slight strength. So the induced magnetic field is negligible. We suppose that the boundary wall of the artery is rigid and the artery has a porous medium of time dependent permeability. Next, the artery is inclined to the vertical and a slip velocity is considered at the stenosed region of the arterial wall. Here, blood is considered as a Newtonian fluid and the respective flow is assumed to be Newtonian. The flow configuration is shown diagrammatically, at the **end** of the **Result and discussion** section.

The geometry of an arterial stenosis is (Nagarani and Sarojamma [25]), as below:

$$\overline{R}\left(\overline{z}\right) = \begin{cases} \overline{L} - \dfrac{\overline{d}_s}{2}\left(1 + \cos\dfrac{\pi \overline{z}}{\overline{d}_0}\right), & \text{for } \left|\overline{z}\right| \leq \overline{d}_0 \\ \overline{L}, & \text{for } \left|\overline{z}\right| > \overline{d}_0 \end{cases} \tag{1}$$

Where $\overline{R}\left(\overline{z}\right)$ is the radius of the artery in the stenosed region, $\overline{L}$ is the constant arterial radius in the non-stenosed region, $\overline{d}_0$ is the half-length of the stenosis and $\overline{d}_s$ is the greatest height of the stenosis such that $\dfrac{\overline{d}_s}{\overline{L}}$ is less than unity for a mild stenosis. Here the radial velocity is very small due to the low Reynolds number flow through the artery with mild stenosis (Nagarani and Sarojamma [25]); hence we do not consider the radial velocity.

From Navier-Stokes equations of motion, the momentum equation governing the flow is reduced in the cylindrical coordinate system $\left(\overline{r}, \overline{\theta}, \overline{z}\right)$ as under:

$$\frac{\partial \bar{u}}{\partial \bar{t}} = \frac{1}{\rho} \bar{F}(\bar{t}) + g\cos\beta - \frac{1}{\rho}\frac{\partial \bar{P}}{\partial \bar{z}} + \upsilon\left(\frac{\partial^2 \bar{u}}{\partial \bar{r}^2} + \frac{1}{\bar{r}}\frac{\partial \bar{u}}{\partial \bar{r}}\right) - \frac{\sigma \bar{u} \bar{B}^2}{\rho} - \frac{\upsilon \bar{u}}{\bar{K_0}} \qquad (2)$$

$$\frac{\partial \bar{P}}{\partial \bar{r}} = -g\rho Sin\beta \qquad (3)$$

Where $\bar{u}$ denotes the velocity along the $\bar{z}$ - axis, $\bar{P}$ the pressure, ρ the density, $\bar{t}$ the time, $\bar{F}(\bar{t})$ the body acceleration, $\bar{B}$ the applied magnetic field in azimuthal ($\bar{\theta}$) direction, υ the kinematic viscosity, σ the electrical conductivity, g the acceleration due to gravity, β the angle of inclination of the artery with the vertical and $\bar{K_0}$ the periodic permeability of the porous medium, such that $\bar{K_0} = \dfrac{\bar{K}}{1 + \varepsilon_k \cos(\bar{\omega_p t})}$, where ε_k is the amplitude of permeability.

Such that the boundary conditions are:

$$\bar{u} = \bar{V_s} \text{ at } \bar{r} = \bar{R}(\bar{z}) \qquad (4)$$

$$\frac{\partial \bar{u}}{\partial \bar{r}} = 0 \text{ at } \bar{r} = 0 \qquad (5)$$

Where $\bar{V_s}$ is the slip velocity at the stenosed region of the arterial wall.

When $\bar{t} > 0$, periodic body acceleration $\bar{F}(\bar{t})$ is levied on the flow and this is expressed as below (Nagarani and Sarojamma [25]):

$$\bar{F}(\bar{t}) = f_0 \cos(\bar{\omega_0} \bar{t} + \theta) \qquad (6)$$

Where $\bar{\omega_0} = 2\pi \bar{F_b}$, f_0 is the amplitude of the body acceleration and $\bar{F_b}$ is the frequency (in Hertz) of body acceleration. Also, θ is the lead angle with respect to the heart action. $\bar{F_b}$ is assume as very small so that the wave effect can be neglected (Nagarani and Sarojamma [25]).

Now, for $\bar{t} \geq 0$, the pressure gradient is considered as:

$$-\frac{\partial \bar{P}(\bar{z},\bar{t})}{\partial \bar{z}} = P_0(\bar{z}) + P_1(\bar{z})\cos(\bar{\omega}_P \bar{t}) \tag{7}$$

Where, $P_0(\bar{z})$ and $P_1(\bar{z})$ are the steady state pressure gradient and the amplitude of the oscillatory part of the pressure gradient. Further, $\bar{\omega}_P = 2\pi \bar{f}_P$ where $\bar{f}_P$ is the pulse rate frequency.

We define the following non-dimensional substitutions:

$$z = \frac{\bar{z}}{\bar{L}}, R(z) = \frac{\bar{R}(\bar{z})}{\bar{L}}, r = \frac{\bar{r}}{\bar{L}}, t = \bar{t}\,\bar{\omega}_P, \omega = \frac{\bar{\omega}_0}{\bar{\omega}_P}, d_s = \frac{\bar{d}_s}{\bar{L}}, u = \frac{4\,\upsilon\,\rho\,\bar{u}}{P_0\,\bar{L}^2},$$

$$B' = \frac{\rho\,g}{P_0}, V_s = \frac{4\,\upsilon\,\rho\,\bar{V}_s}{P_0\,\bar{L}^2}, \tau = \frac{2\,\bar{\tau}}{P_0\,\bar{L}}, \varepsilon^2 = \frac{\bar{L}^2\,\bar{\omega}_P}{\upsilon}, \varepsilon_0 = \frac{P_1}{P_0}, B = \frac{f_0}{P_0},$$

$$M = \frac{\sigma\,\bar{B}^2\,\bar{L}^2}{\upsilon\,\rho}, K = \frac{\bar{K}}{\bar{L}^2}, d_0 = \frac{\bar{d}_0}{\bar{L}}, \mu_E = \frac{\bar{\mu}_E}{8\,\upsilon\,\rho}, \tag{8}$$

Where ε, M, K and d_s are respectively the Pulsatile Reynolds number or the Womersley frequency parameter, Hartmann number or magnetic parameter, the permeability parameter and the dimensionless height of the stenosis. The remaining quantities relevant to this problem are described at their appropriate places.

We use the quantities of (8) into (1), (2), (4), (5), (6) and (7) and then simplifying, we get the following in non-dimensional forms:

Non-dimensional form of the geometry of arterial stenosis is:

$$R(z) = \begin{cases} 1 - \dfrac{d_s}{2}\left(1 + \cos\dfrac{\pi z}{d_0}\right), & \text{for } |z| \leq d_0 \\ 1, & \text{for } |z| > d_0 \end{cases} \tag{9}$$

Momentum equation:

$$\varepsilon^2 \frac{\partial u}{\partial t} = 4\left\{B\cos(\omega t+\theta)+B'\cos\beta+(1+\varepsilon_0\cos t)\right\}$$

$$+ \frac{1}{r}\frac{\partial}{\partial r}\left(r\frac{\partial u}{\partial r}\right)-\left(M+\frac{1+\varepsilon_k\cos t}{K}\right)u \tag{10}$$

Subject to the following non-dimensional boundary conditions:

$$u=V_s \text{ at } r=R \tag{11}$$

$$\frac{\partial u}{\partial r}=0 \text{ at } r=0 \tag{12}$$

2.3 Method of Solution

We have solved the problem with the aid of multiparameter perturbation technique. For perturbation technique, let the Pulsatile Reynolds number ε to be extremely small, as a consequence the velocity u may be represented by the following series:

$$u(z,r,t)=v_0(z,r,t)+\varepsilon^2 v_1(z,r,t)+....... \tag{13}$$

Putting (13) in (10), using the boundary condition (11) and (12) and equating the similar coefficients of ε and then neglecting the terms having higher powers of ε, we get:

$$0=4h(t)+\frac{1}{r}\frac{\partial}{\partial r}\left(r\frac{\partial v_0}{\partial r}\right)-\left(M+\frac{1+\varepsilon_k\cos t}{K}\right)v_0 \tag{14}$$

$$\frac{\partial v_0}{\partial t}=\frac{1}{r}\frac{\partial}{\partial r}\left(r\frac{\partial v_1}{\partial r}\right)-\left(M+\frac{1+\varepsilon_k\cos t}{K}\right)v_1 \tag{15}$$

Where $h(t)=B\cos(\omega t+\theta)+B'\cos\beta+(1+\varepsilon_0\cos t)$.

Taking ε_k as perturbation parameter, we assume:

$$v_0=v_{00}+\varepsilon_k v_{01} \tag{16}$$

$$v_1=v_{10}+\varepsilon_k v_{11} \tag{17}$$

Putting (16) and (17) in (14), (15) and equating the coefficients of ε_k^0 and ε_k^1 and then neglecting the terms containing higher powers of ε_k, we get

8

$$0 = 4h(t) + \frac{1}{r}\frac{\partial}{\partial r}\left(r\frac{\partial v_{00}}{\partial r}\right) - \left(M + \frac{1}{K}\right)v_{00} \tag{18}$$

$$0 = \frac{1}{r}\frac{\partial}{\partial r}\left(r\frac{\partial v_{01}}{\partial r}\right) - \left[\frac{\cos t}{K}v_{00} + \left(M + \frac{1}{K}\right)v_{01}\right] \tag{19}$$

$$\frac{\partial v_{00}}{\partial t} = \frac{1}{r}\frac{\partial}{\partial r}\left(r\frac{\partial v_{10}}{\partial r}\right) - \left(M + \frac{1}{K}\right)v_{10} \tag{20}$$

$$\frac{\partial v_{01}}{\partial t} = \frac{1}{r}\frac{\partial}{\partial r}\left(r\frac{\partial v_{11}}{\partial r}\right) - \left[\frac{\cos t}{K}v_{10} + \left(M + \frac{1}{K}\right)v_{11}\right] \tag{21}$$

The subsequent boundary conditions are:

$$v_{00} = V_s, \ v_{01} = 0, v_{10} = 0, \ v_{11} = 0 \text{ at } r = R \tag{22}$$

$$\frac{\partial v_{00}}{\partial r} = 0 \ , \ \frac{\partial v_{01}}{\partial r} = 0, \frac{\partial v_{10}}{\partial r} = 0 \ , \ \frac{\partial v_{11}}{\partial r} = 0 \text{ at } r = 0 \tag{23}$$

The solution of the equations (18), (19), (20) and (21) with respect to the boundary conditions (22), (23) are as follows:

$$v_{00} = \left[c_1 J_0\left(ri\sqrt{K_1}\right) + \frac{4}{K_1}\right]h(t), \text{ where } c_1 = \frac{\left[\frac{V_s}{h(t)} - \frac{4}{K_1}\right]}{J_0\left(Ri\sqrt{K_1}\right)},$$

$v_{10} = V(r)h'(t)$, where $h'(t)$ represents the derivative of $h(t)$ with respect to t;

$$V(r) = c_1 J_0\left(ri\sqrt{K_1}\right)\left[\frac{r^2}{4} + \psi(r) + c_2\right] - \frac{4}{K_1^2};$$

$$\text{Where, } \psi(r) = -\frac{1}{2K_1}\left[\frac{ri\sqrt{K_1} J_1\left(ri\sqrt{K_1}\right)}{J_0\left(ri\sqrt{K_1}\right)} + \frac{r^2 K_1}{2}\right],$$

$$c_2 = \frac{4}{K_1^2 c_1 J_0\left(Ri\sqrt{K_1}\right)} - \frac{R^2}{4} - \psi(R),$$

$$v_{01} = \left[\cos t\, h(t)\, \frac{V(r)}{K}\right],$$

$$v_{11} = \left[J_0\left(r\,i\sqrt{K_1} \right) \overline{z}(r) + \frac{4}{K\,K_1^3} \right] \left(2\cos t\; h'(t) - h(t)\sin t \right),$$

Where $\;K_1 = M + \dfrac{1}{K}\,,$

$$\overline{z}(r) = \left\{ \frac{c_1\,r^4}{32\,K} + \frac{c_1\,c_2\,r^2}{4\,K} + \left(\frac{c_1\,r^2}{4\,K} + \frac{c_1\,c_2}{K} - \frac{c_1}{2\,K\,K_1} \right) \psi(r) \right.$$

$$\left. + \frac{c_1}{2\,K}\left(\psi(r) \right)^2 + \frac{c_1\,i\sqrt{K_1}}{4\,K\,K_1}\,\psi_2(r) + \frac{c_1\,i\sqrt{K_1}}{4\,K\,K_1}\,\psi_3(r) \right\} + \overline{B}\,,$$

And

$$\overline{B} = \left\{ -\frac{4}{K\,K_1^3\,J_0\left(R\,i\sqrt{K_1} \right)} - \frac{c_1\,R^4}{32\,K} - \frac{c_1\,c_2\,R^2}{4\,K} - \left(\frac{c_1\,R^2}{4\,K} + \frac{c_1\,c_2}{K} - \frac{c_1}{2\,K\,K_1} \right) \psi(R) \right.$$

$$\left. - \frac{c_1}{2\,K}\left(\psi(R) \right)^2 - \frac{c_1\,i\sqrt{K_1}}{4\,K\,K_1}\,\psi_2(R) - \frac{c_1\,i\sqrt{K_1}}{4\,K\,K_1}\,\psi_3(R) \right\},$$

$$\psi_2(r) = \frac{r^2\,i}{\sqrt{K_1}}\,Log\left(J_0\left(r\,i\sqrt{K_1} \right) \right) - \frac{2\,i\sqrt{K_1}}{K_1}\int_0^r x\,Log\left(J_0\left(x\,i\sqrt{K_1} \right) \right) dx,$$

$$\psi_3(r) = -\frac{i\,r^2\,J_1^{\,2}\left(r\,i\sqrt{K_1} \right)}{2\sqrt{K_1}\,J_0^{\,2}\left(r\,i\sqrt{K_1} \right)} - \frac{i\,r^2}{\sqrt{K_1}}\,Log\left(J_0\left(r\,i\sqrt{K_1} \right) \right)$$

$$+ \frac{2\,i}{\sqrt{K_1}}\int_0^r x\,Log\left(J_0\left(x\,i\sqrt{K_1} \right) \right) dx \quad .$$

Consequently, the non-dimensional axial velocity $u(z,r,t)$ is given by:

$$u(z,r,t) = v_{00} + \varepsilon_k\,v_{01} + \varepsilon^2\left(v_{10} + \varepsilon_k\,v_{11} \right)$$

3.1 Non-dimensional Wall Shear Stress

Assuming a rigid arterial wall, the dimensionless wall shear stress τ at $r = R$ is as under:

$$\tau = \frac{2\bar{\tau}}{P_0 \bar{L}},$$

Where $\bar{\tau} = -\upsilon \rho \left(\dfrac{\partial \bar{u}}{\partial \bar{r}} \right)_{\bar{r}=\bar{R}}$ is the dimensional wall shear stress at $\bar{r}=\bar{R}$.

Consequently, we get:

$$\tau = -\frac{1}{2}\left(\frac{\partial u}{\partial r}\right)_{r=R} = -\frac{1}{2}\left[\left(\frac{\partial v_{00}}{\partial r}\right)+\varepsilon_k\left(\frac{\partial v_{01}}{\partial r}\right)+\varepsilon^2\left(\frac{\partial v_{10}}{\partial r}\right)+\varepsilon^2\varepsilon_k\left(\frac{\partial v_{11}}{\partial r}\right)\right]_{r=R},$$

Where $\dfrac{\partial v_{00}}{\partial r} = -c_1 i \sqrt{K_1}\, J_1\!\left(r i \sqrt{K_1}\right) h(t)$,

And $\dfrac{\partial v_{10}}{\partial r} = h'(t) V'(r)$,

Where $V'(r) = \left[-c_1 c_2 i \sqrt{K_1}\, J_1\!\left(r i \sqrt{K_1}\right) + \dfrac{c_1}{2} r J_0\!\left(r i \sqrt{K_1}\right) \right]$.

Again $\dfrac{\partial v_{01}}{\partial r} = \cos t\; h(t)\, \dfrac{V'(r)}{K}$,

And $\dfrac{\partial v_{11}}{\partial r} = \left(2\cos t\, h'(t) - h(t)\sin t\right)\left[\bar{z}'(r) J_0\!\left(r i \sqrt{K_1}\right) - \bar{z}(r)\, i \sqrt{K_1}\, J_1\!\left(r i \sqrt{K_1}\right)\right]$,

Where $\bar{z}'(r) = \dfrac{c_1 c_2 r}{2K} + \left(\dfrac{c_1 c_2}{2K} - \dfrac{c_1}{4KK_1} \right) \dfrac{r J_1^{\,2}\!\left(r i \sqrt{K_1}\right)}{J_0^{\,2}\!\left(r i \sqrt{K_1}\right)}.$

3.2 Non-dimensional Volumetric Flow Rate

The non-dimensional volumetric flow rate $Q(z,t)$ may be defined as follows:

$$Q(z,t) = \frac{8 \upsilon \rho\, \bar{Q}(\bar{z},\bar{t})}{\pi \bar{L}^4 P_0}, \text{ where } \bar{Q}(\bar{z},\bar{t}) \text{ is the dimensional volumetric flow rate}$$

and is given by $\bar{Q}(\bar{z},\bar{t}) = 2\pi \displaystyle\int_0^{\bar{R}} \bar{r}\, \bar{u}(\bar{z}, \bar{r}, \bar{t})\, d\bar{r}$.

Consequently, $Q(z,t) = 4 \int_0^R r\, u(z, r, t)\, dr = 4\left(Q_{00} + \varepsilon_k\, Q_{01} + \varepsilon^2\, Q_{10} + \varepsilon^2\, \varepsilon_k\, Q_{11} \right)$,

Where we define the following:

$$Q_{00} = \int_0^R r\, v_{00}\, dr = -\frac{c_1\, h(t)\, R i \sqrt{K_1}\, J_1\left(R i \sqrt{K_1}\right)}{K_1} + \frac{2 h(t) R^2}{K_1} \;;$$

$$Q_{01} = \int_0^R r\, v_{01}\, dr = \frac{\cos t\, h(t)}{K} \left[\frac{R^2 V(R)}{2} - \frac{c_1 R^2 J_2\left(R i \sqrt{K_1}\right)}{2} \left(\frac{1}{K_1} - c_2 \right) \right.$$
$$\left. + \frac{c_1 R^3 i \sqrt{K_1}\, J_1\left(R i \sqrt{K_1}\right)}{4 K_1} \right] ;$$

$$Q_{10} = \int_0^R r\, v_{10}\, dr = h'(t) \left[\frac{R^2 V(R)}{2} - \frac{c_1 R^2 J_2\left(R i \sqrt{K_1}\right)}{2} \left(\frac{1}{K_1} - c_2 \right) \right.$$
$$\left. + \frac{c_1 R^3 i \sqrt{K_1}\, J_1\left(R i \sqrt{K_1}\right)}{4 K_1} \right] ;$$

$$Q_{11} = \int_0^R r\, v_{11}\, dr = \left(2\cos t\, h'(t) - h(t)\, \sin t \right) \left[-\frac{\overline{z}(R) R i \sqrt{K_1}\, J_1\left(R i \sqrt{K_1}\right)}{K_1} \right.$$
$$\left. + \frac{i \sqrt{K_1}\, \psi_4(R)}{K_1} + \frac{2 R^2}{K K_1^3} \right],$$

Where,

$$\psi_4(R) = \frac{c_1 R^2 i\, J_2\left(R i \sqrt{K_1}\right)}{2 K \sqrt{K_1}} \left(c_2 - \frac{1}{K_1} \right) + \left(\frac{1}{2 K_1} - c_2 \right) \frac{c_1 R^2 i\, J_1^2\left(R i \sqrt{K_1}\right)}{2 K \sqrt{K_1}\, J_0\left(R i \sqrt{K_1}\right)} .$$

3.3 Dimensionless Effective Viscosity

The effective viscosity $\overline{\mu}_E$ in dimensional form may be defined as under, following Pennington and Cowin [28]:

$$\overline{\mu}_E = \frac{\pi \left(-\dfrac{\partial \overline{P}\left(\overline{z},\overline{t}\right)}{\partial \overline{z}} \right)\left(\overline{R}\left(\overline{z}\right)\right)^4}{\overline{Q}\left(\overline{z},\overline{t}\right)}$$

$$\Rightarrow \mu_E = \frac{\left(1+\varepsilon_0 \cos t\right) R^4}{Q\left(z,t\right)}$$

Where μ_E is the non-dimensional effective viscosity.

4 Result and discussion

In order to get an insight into the biological and physical aspects of this problem, we obtain the profiles of the axial velocity, wall shear stress, volumetric flow rate and the effective viscosity, and we examine their behaviors under the influence of the various non-dimensional parameters relevant to this problem. The data-tabulation involved in this problem is carried out with the aid of Wolfram Mathematica. Unless otherwise indicated, for the data-tabulation, we take

$z = 0.2,\quad d_0 = 0.3\ ,\ \varepsilon = 0.2\ ,\ \varepsilon_k = 0.2\ ,\ \theta = \dfrac{\pi}{3}\ ,\ B' = 0.5,\quad \omega = \dfrac{\pi}{8},\quad d_s = 0.25,$

$R = 0.9375,\ \ t = 3,\quad \varepsilon_0 = 0.5,\ B = 0.5.$ Clearly, $r \in [0, R]$ and using (9) and then noting that $|z| < d_0$ for the aforementioned choice of z, d_0, we find that $R = 0.9375$. Thus, for our choice of $z, d_0,\ \ r \in [0,\ 0.9375]$. It may be mentioned that the values of t (involved in the following figures 5 to 15, and then from the figures 17 to 19 and in the table 1) range from 0 to 2π. This is done to incorporate one **complete period** (**full cycle**) of the **pulsatile pressure gradient** and the **periodic body acceleration**.
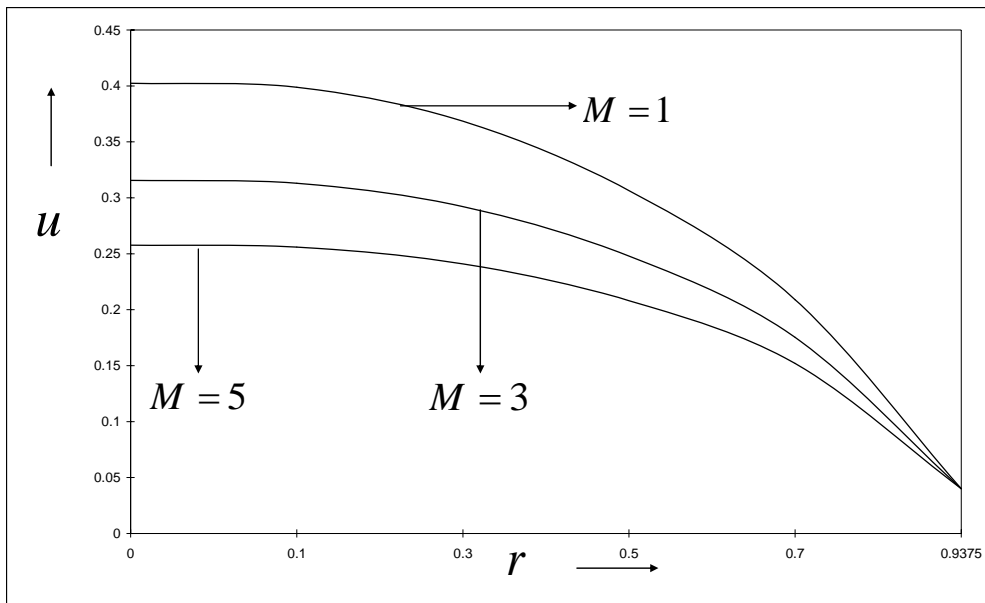
Figure 1: Velocity u against r, under the effect of M for $K = 1,\ \beta = \dfrac{\pi}{4},\ V_S = 0.04$.
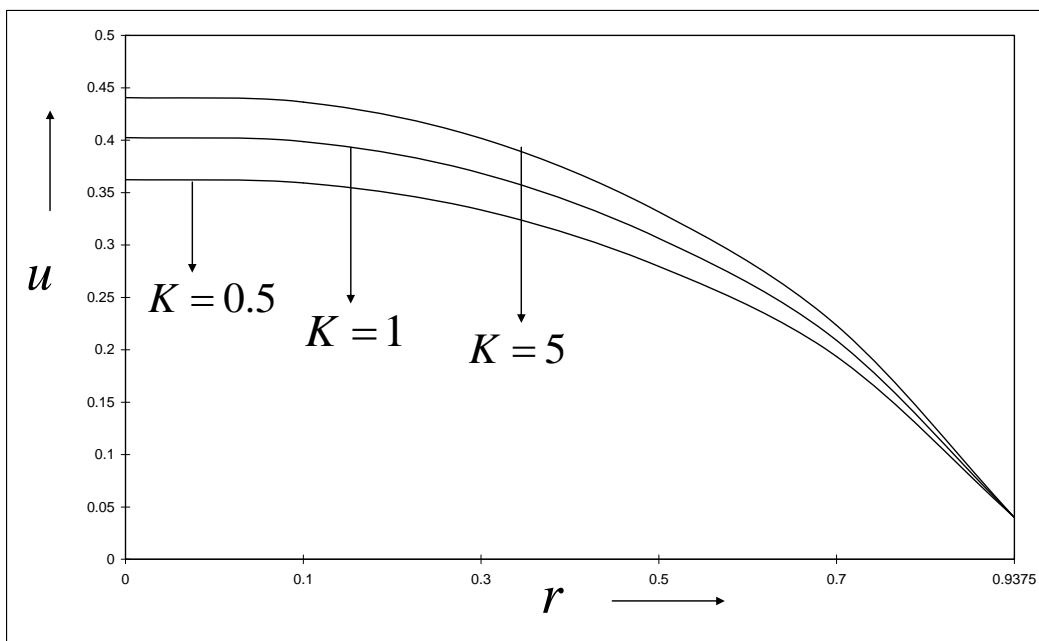
Figure 2: Velocity u against r, under the effect of K for

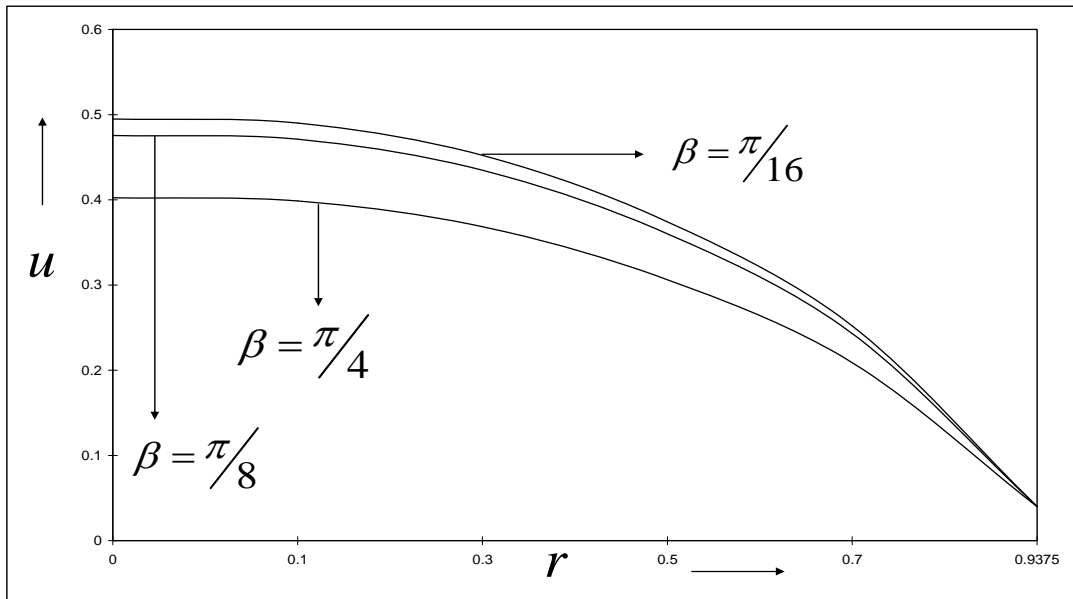$M = 1,\ \beta = \dfrac{\pi}{4}, V_S = 0.04$.

Figure 3: Velocity u against r, under the effect of β for
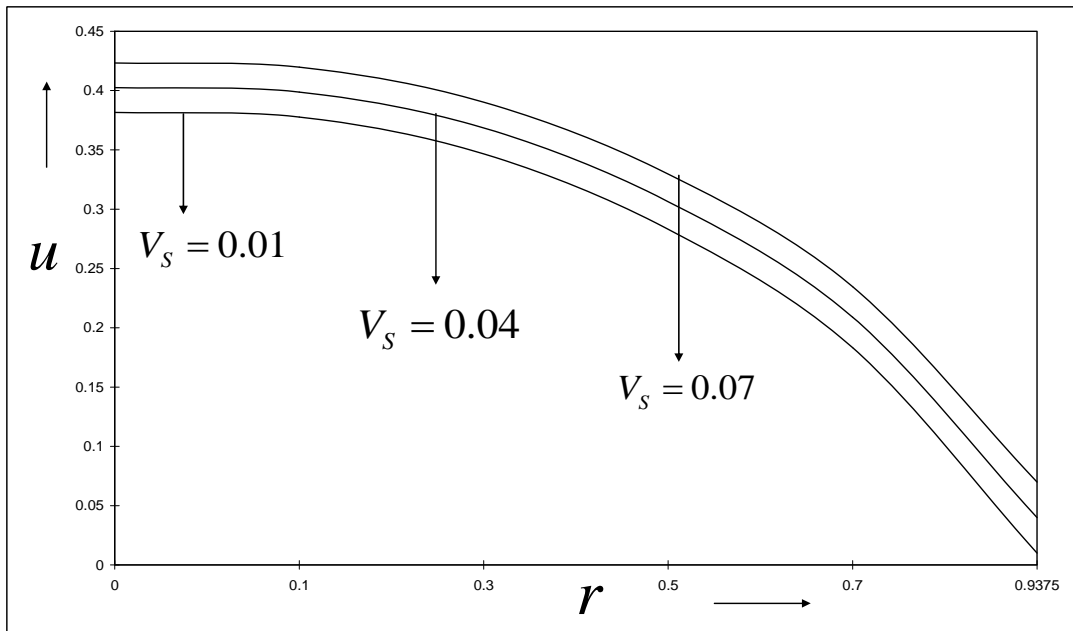$M = 1,\ K = 1, V_S = 0.04$.

Figure 4: Velocity u against r, under the effect of V_S for

$$M = 1,\ K = 1,\ \beta = \frac{\pi}{4}.$$

From the figures 1 to 4, it is evident that the blood flow speed increases as

the porosity and the slip velocity rises. Thus, the possible imposition of slip velocity at the stenosed wall and greater porosity may enhance the blood flow through the stenosed section of the artery. These observations agree with well known results and this validates our flow model as physically realizable.

Again, it is seen that the blood flow speed decreases with the imposition of the magnetic field and an increase in the angle of inclination. The application of the azimuthal magnetic field leads to the development of Lorentz force that in turn decelerates the flow. Hence, the azimuthal magnetic field can be used to control the blood flow through stenosed artery. Moreover, it is obvious from the **flow figure** that a rise in β (inclination) would imply lesser assistance from gravity towards the blood flow that is occurring in the downward direction along the z-axis. Naturally then, a rise in β (inclination) will cause a reduction in the blood flow speed.
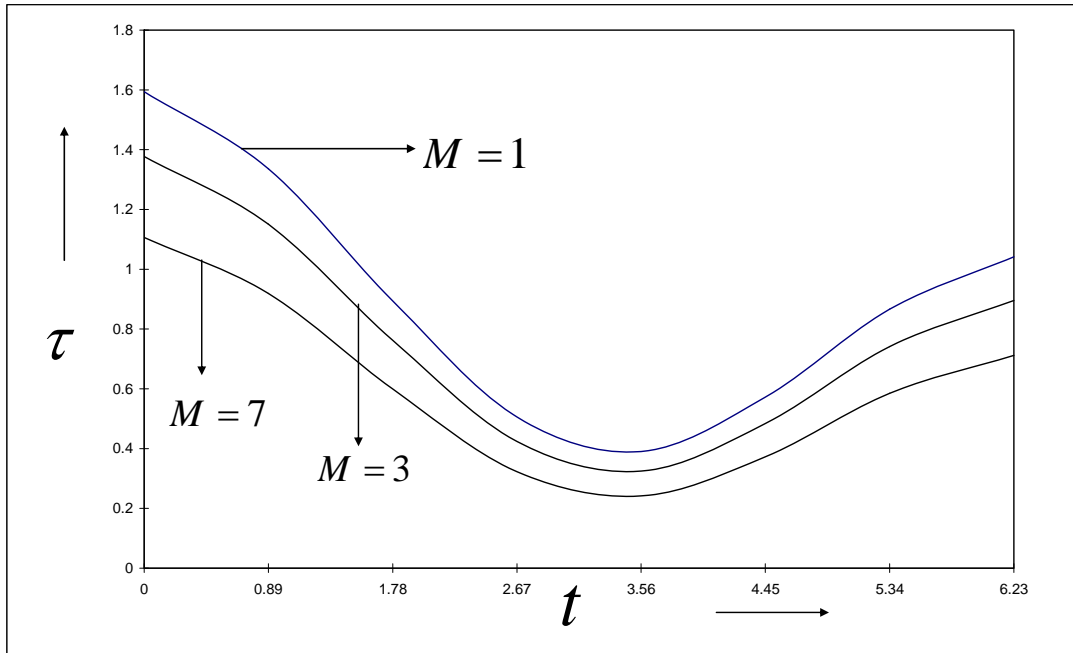
Figure 5: Shear stress τ against t under the effect of M, for
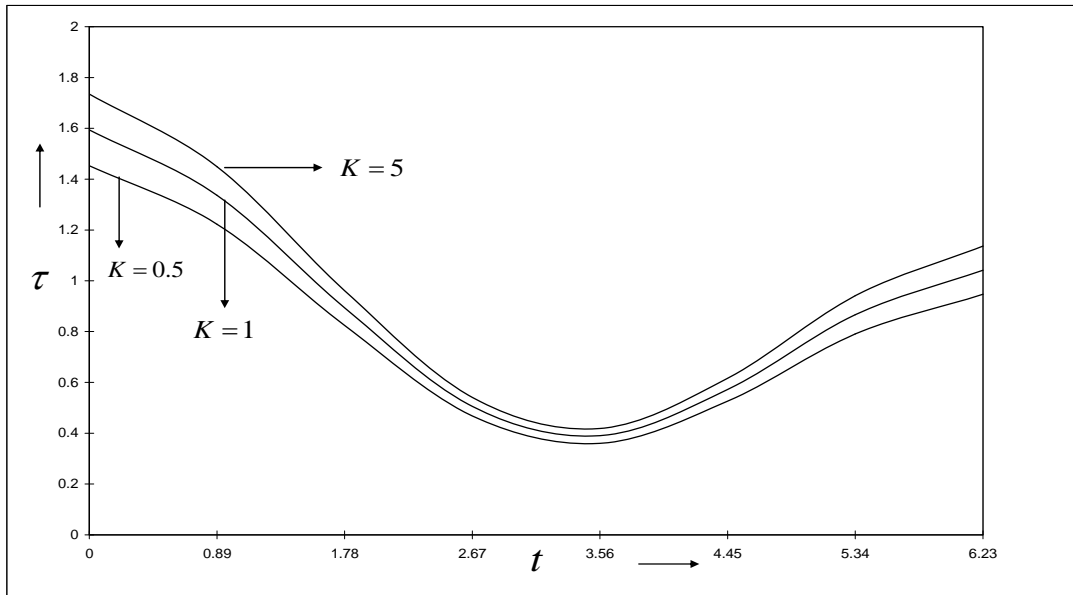
$$K = 1, \ \beta = \frac{\pi}{4}, V_S = 0.04.$$

Figure 6: Shear stress τ against t under the effect of K, for

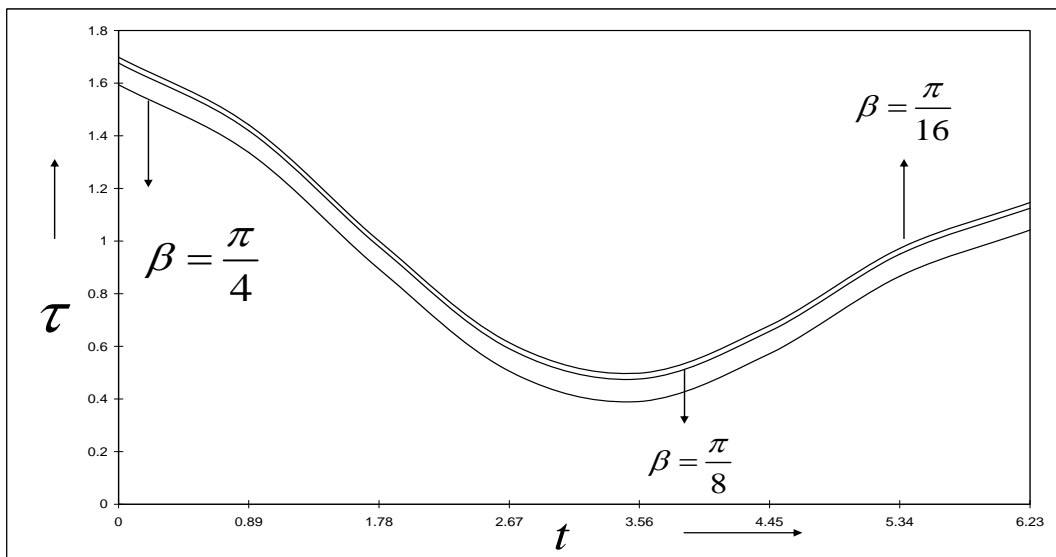$$M = 1, \ \beta = \frac{\pi}{4}, V_S = 0.04 \ .$$

Figure 7: Shear stress τ against t under the effect of β, for

$$M = 1, \ K = 1, V_S = 0.04 \ .$$

t	$\tau\left(V_S = 0.01\right)$	$\tau\left(V_S = 0.04\right)$	$\tau\left(V_S = 0.07\right)$
0	1.6064	1.59376	1.58113
$\dfrac{2\pi}{7}$	1.34861	1.33639	1.32417
$\dfrac{4\pi}{7}$	0.905096	0.893745	0.882394
$\dfrac{6\pi}{7}$	0.516211	0.505537	0.494863
$\dfrac{8\pi}{7}$	0.401152	0.390351	0.37955
$\dfrac{10\pi}{7}$	0.583814	0.572294	0.560774
$\dfrac{12\pi}{7}$	0.878957	0.866647	0.854337
2π	1.05463	1.04197	1.02931

Table 1: Shear stress τ against t under the effect of V_S, for $M = 1, K = 1, \beta = \dfrac{\pi}{4}$.

The figures 5, 6 and 7 and the table 1 respectively show the behavior of wall shear stress under the influence of magnetic field, porosity, inclination and the slip velocity. It is observed from figure 6 that a rise in the porosity of the medium leads to an increase in the wall shear stress at the stenosed section of the arterial wall. This may be attributed to the fact that the blood flow speed registers a rise as the porosity increases. Consequently, the shear stress also increases.

Again, it is inferred from the figures 5, 7 and table 1 respectively that the wall shear stress at the stenosed section exhibits a decrease with the increase in each of magnetic field, inclination and slip velocity. We may recall that the blood flow speed registers a fall with the imposition of the azimuthal magnetic field and an increase in the inclination angle. Subsequently, the wall shear stress decreases too. Moreover, it is seen from figures 5, 6 and 7 and table 1 that the wall shear stress first decreases and then again increases against dimensionless time t. This is

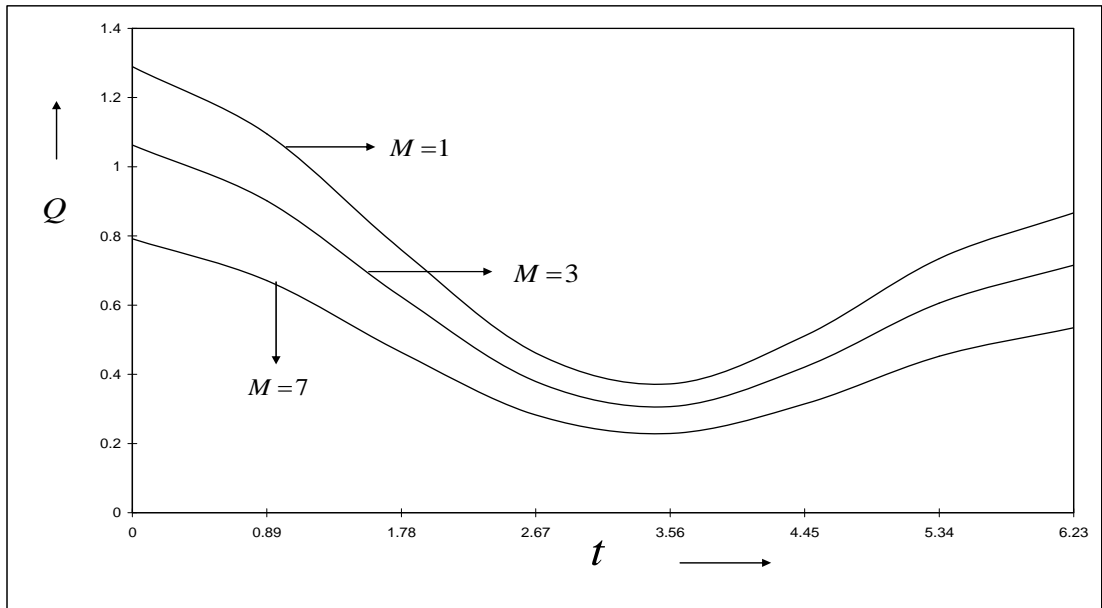due to the periodic nature of the pulsatile pressure gradient associated with this blood flow model.

Figure 8: Volumetric flux Q against t under the effect of M, for
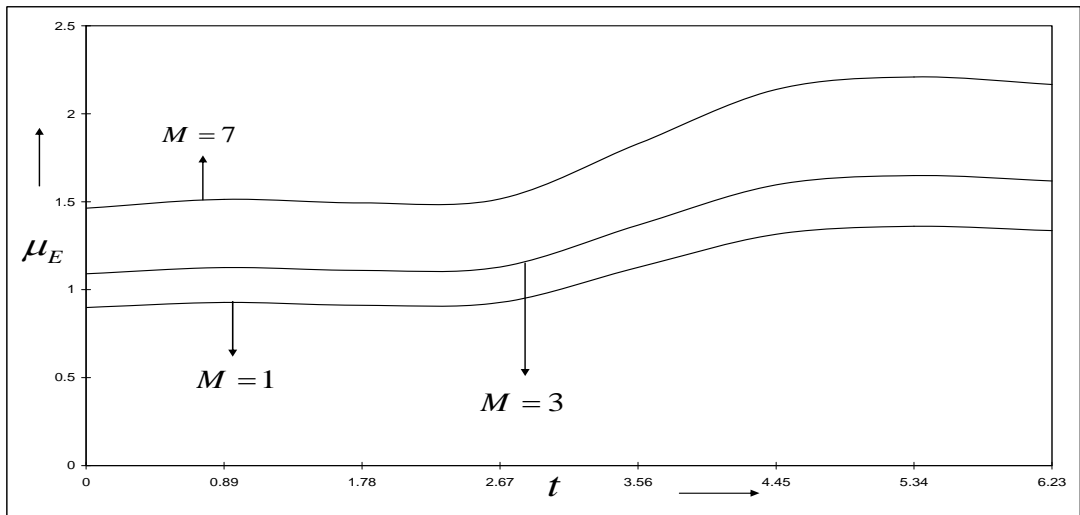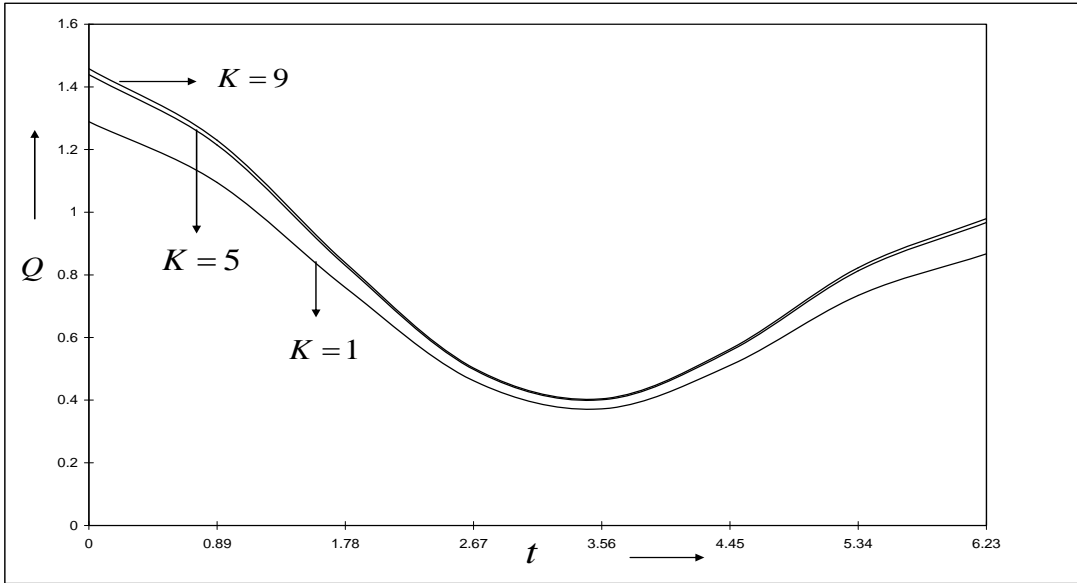
$$K = 1,\ \beta = \frac{\pi}{4}, V_S = 0.04\ .$$

Figure 9: Effective viscosity μ_E against t under the effect of M,

for $K = 1,\ \beta = \frac{\pi}{4}, V_S = 0.04\ .$

Figure 10: Volumetric flux Q against t under the effect of K, for
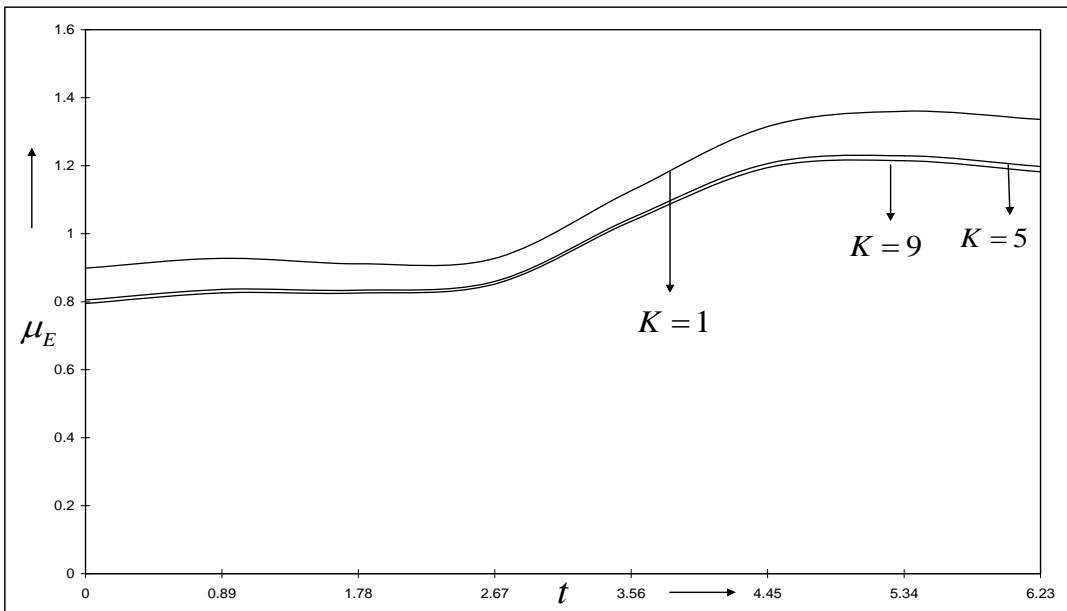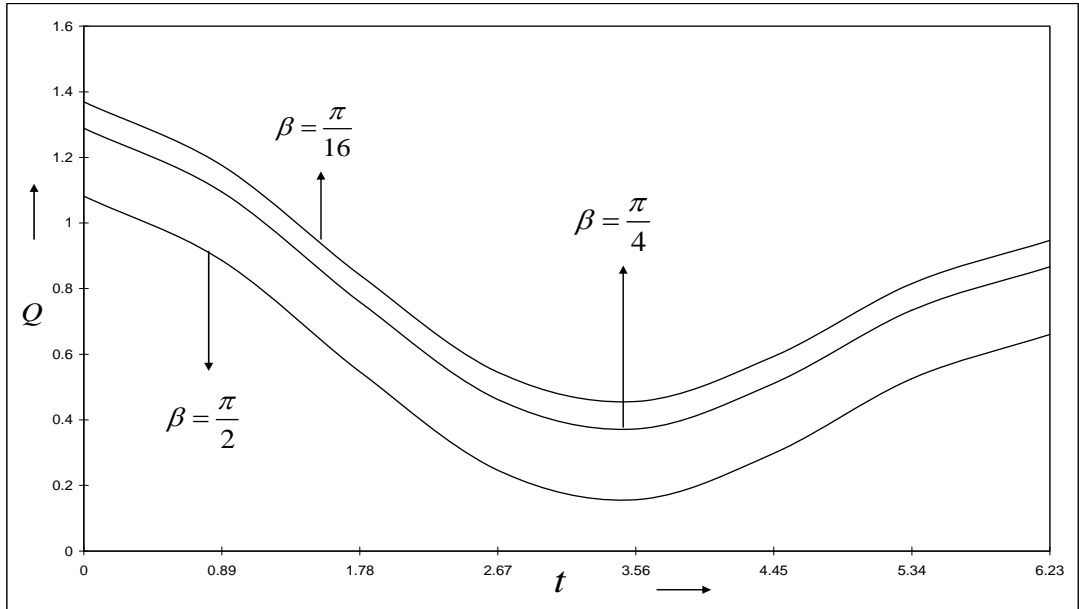
$$M = 1,\ \beta = \frac{\pi}{4},\ V_S = 0.04 .$$

Figure 11: Effective viscosity μ_E against t under the effect of K,

for $M = 1,\ \beta = \frac{\pi}{4},\ V_S = 0.04 .$

Figure 12: Volumetric flux Q against t under the effect of β, for
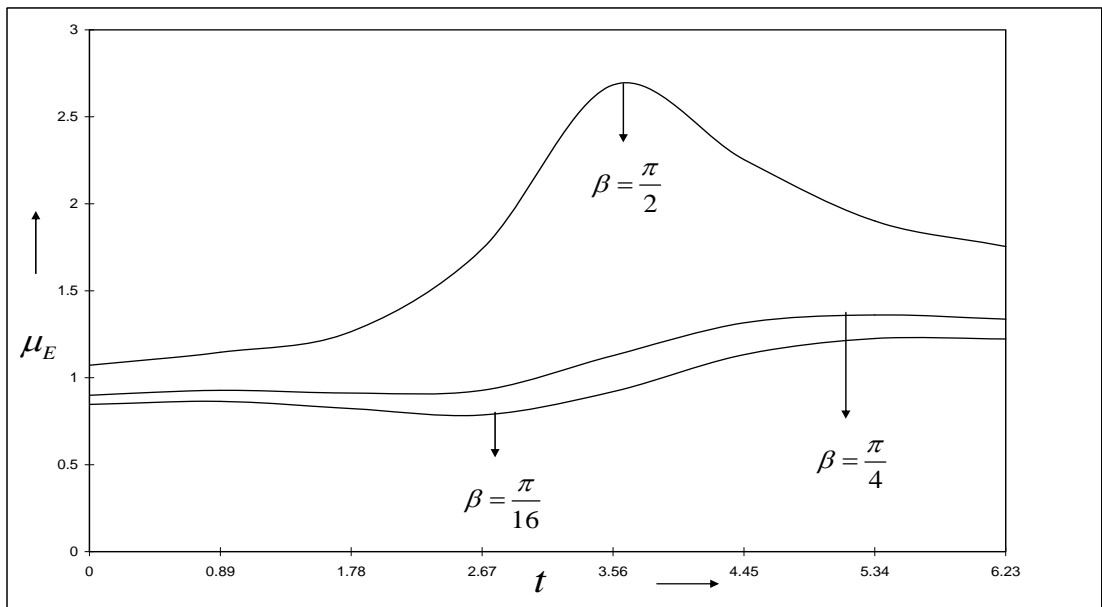
$M = 1,\ K = 1, V_S = 0.04$.

Figure 13: Effective viscosity μ_E against t under the effect of β, for
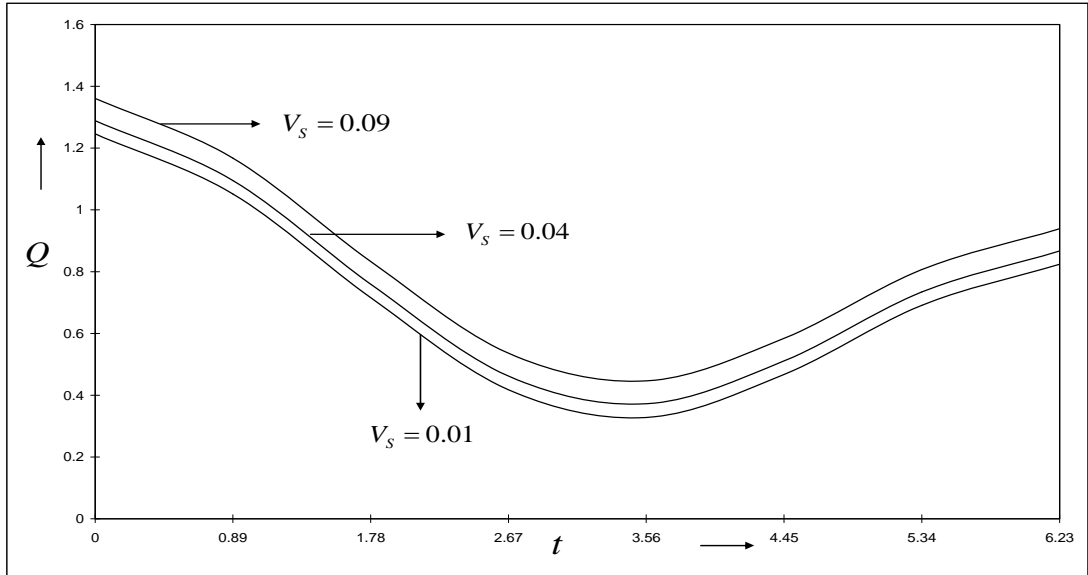
$M = 1,\ K = 1, V_S = 0.04$.

Figure 14: Volumetric flux Q against t under the effect of V_S, for
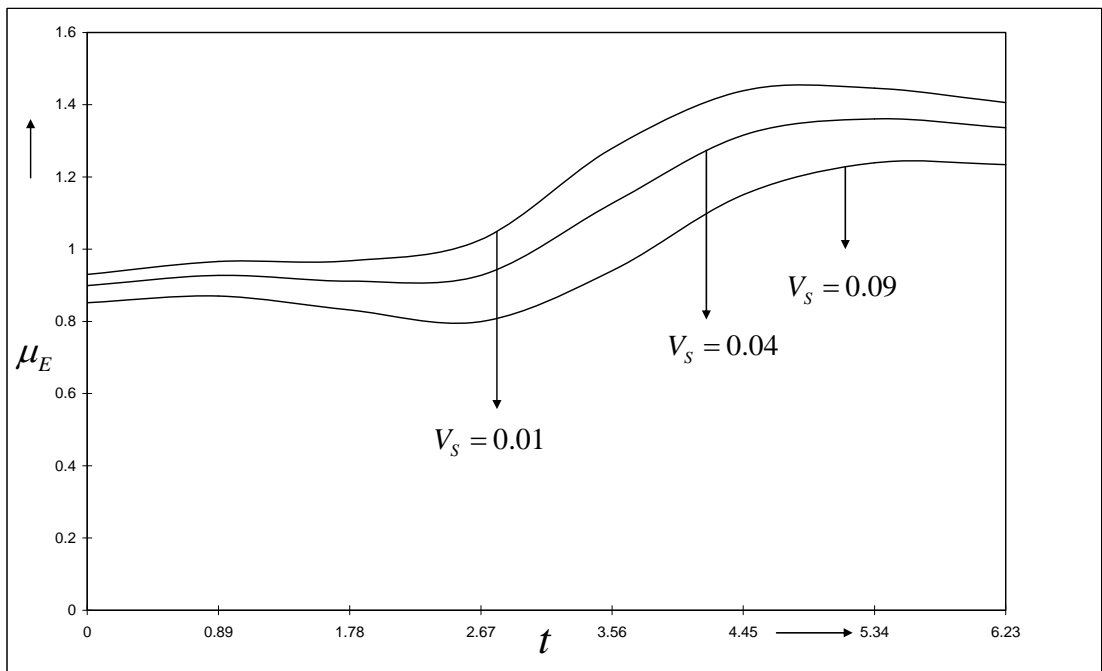
$$M = 1,\ K = 1,\ \beta = \frac{\pi}{4}.$$

Figure 15: Effective viscosity μ_E against t under the effect of V_S, for

$$M = 1,\ K = 1,\ \beta = \frac{\pi}{4}.$$

The figures 8 to 15 portray how the dimensionless volumetric flux Q and the non-dimensional effective viscosity μ_E are affected by the magnetic field (M), porosity (K), inclination (β) and the velocity slip (V_S). From these figures, it is observed that the imposition of the azimuthal magnetic field or an increase in the inclination β decreases the volumetric flux but increases the effective viscosity. On the other hand, a growth in the porosity or the slip velocity leads to a rise in the volumetric flux but causes the effective viscosity to decrease. The perturbed nature of the profiles for the effective viscosity and the volumetric flux against t may be attributed to the pulsatile nature of blood flow owing to the presence of a time dependent pressure gradient.

For the following figures 16 to 19, unless otherwise indicated, we assume that $z = 0.2$, $d_0 = 0.3$, $\varepsilon = 0.2$, $\varepsilon_k = 0.2$, $\theta = \dfrac{\pi}{3}$, $\omega = \dfrac{\pi}{8}$, $d_s = 0.25$, $R = 0.9375$, $t = 3$, $\varepsilon_0 = 0.5$.
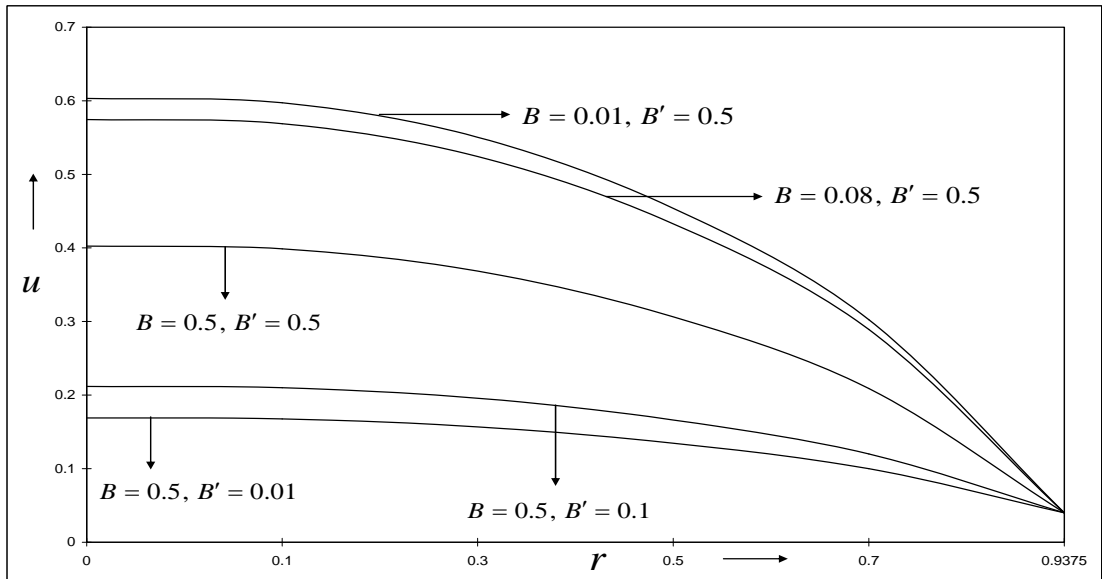

Figure 16: Velocity u versus r, under B, B' for

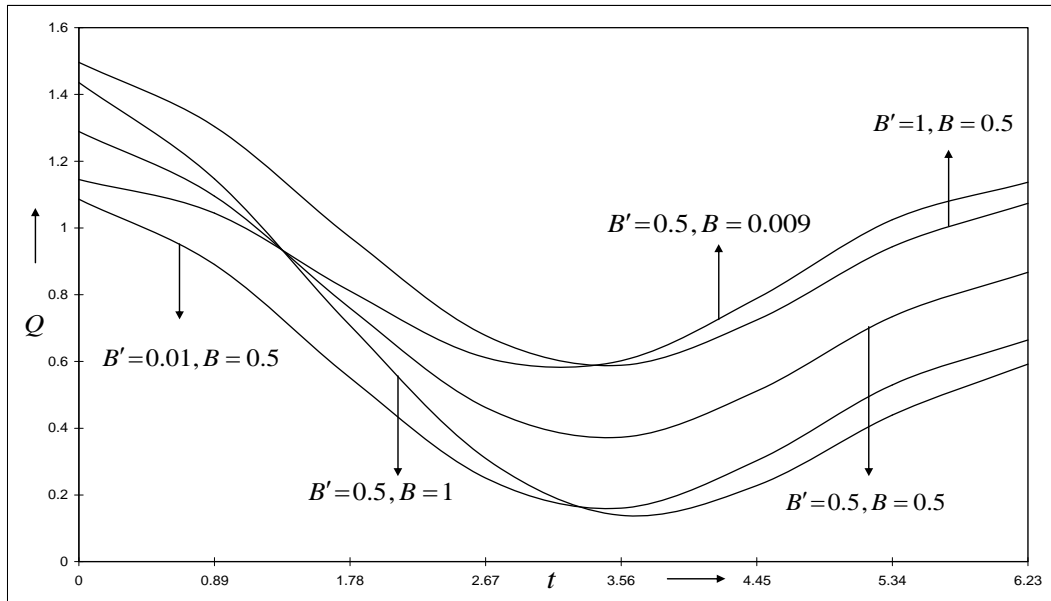$$K = 1,\ \beta = \frac{\pi}{4}, V_S = 0.04,\ M = 1,\ t = 3.$$

Figure 17: Volumetric flux Q versus t, under B, B' for

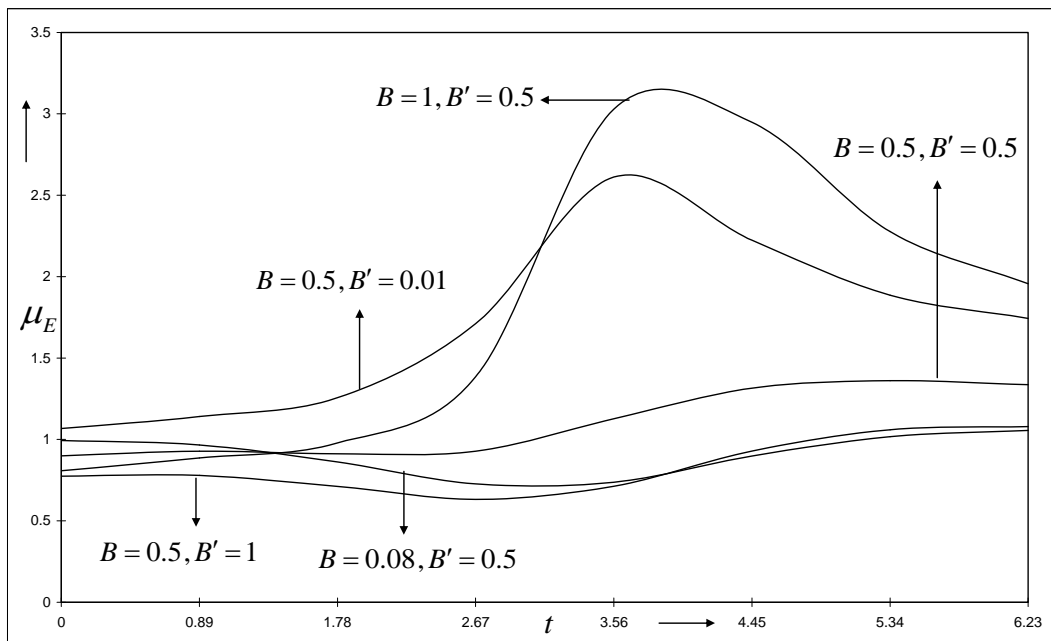$$K = 1, \; \beta = \frac{\pi}{4}, V_S = 0.04, \; M = 1.$$

Figure 18: Effective viscosity μ_E versus t, under B, B' for

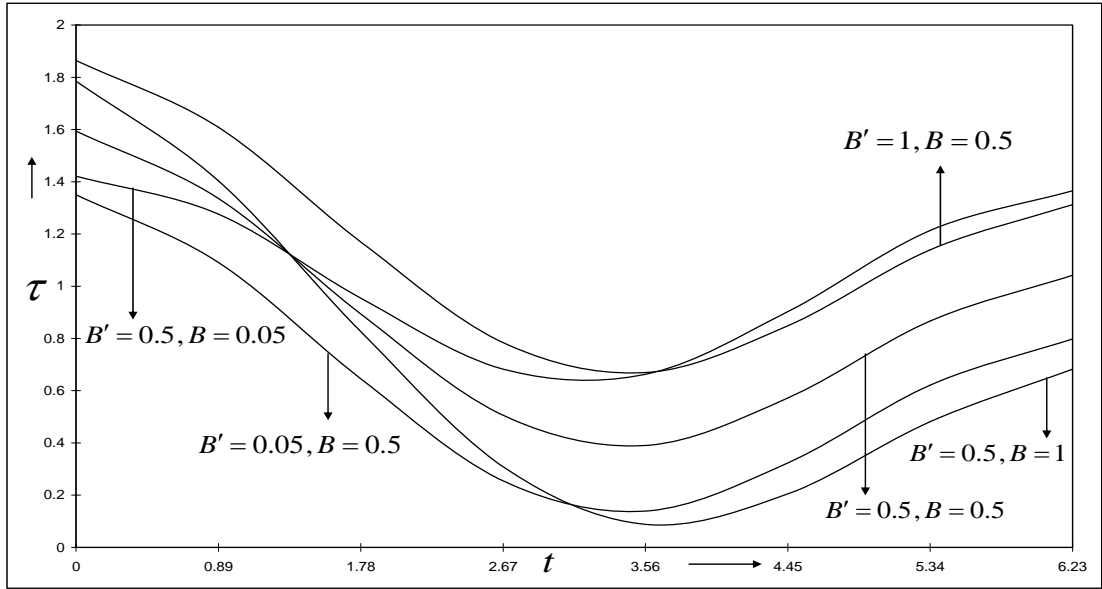$$K = 1, \; \beta = \frac{\pi}{4}, V_S = 0.04, \; M = 1.$$

Figure 19: Shear stress τ versus t, under B, B' for

$$K = 1, \ \beta = \frac{\pi}{4}, V_S = 0.04, \ M = 1.$$

The figures 16 to 19 exhibit the influence of the parameters B and B' on the axial velocity u, the volumetric flux Q, the effective viscosity μ_E and the shear stress τ respectively. It may be noted from the non-dimensional substitutions that B denotes the relative effect of body acceleration over the steady state pressure force. Further, B' signifies the relative effect of gravitational body force (per unit volume of blood) over the steady state pressure force. We observe from figure 16 that the axial velocity u decreases as B increases, whereas u exhibits a growth when B' rises. From figure 17 we note that the volumetric flux Q increases for small time t and decreases for large time t as B rises. The same figure indicates a growth in Q as B' increases for all time t. Figure 18 shows that a rise in B leads to a fall in effective viscosity μ_E for small time t, but μ_E increases for large values of t. The same figure also depicts a decay in μ_E as B' registers a growth for all values of time t. Figure 19 portrays decay in shear stress τ for large time t and

a growth in τ for small time t as B increases. However, τ registers a growth for all time t, as B' increases.
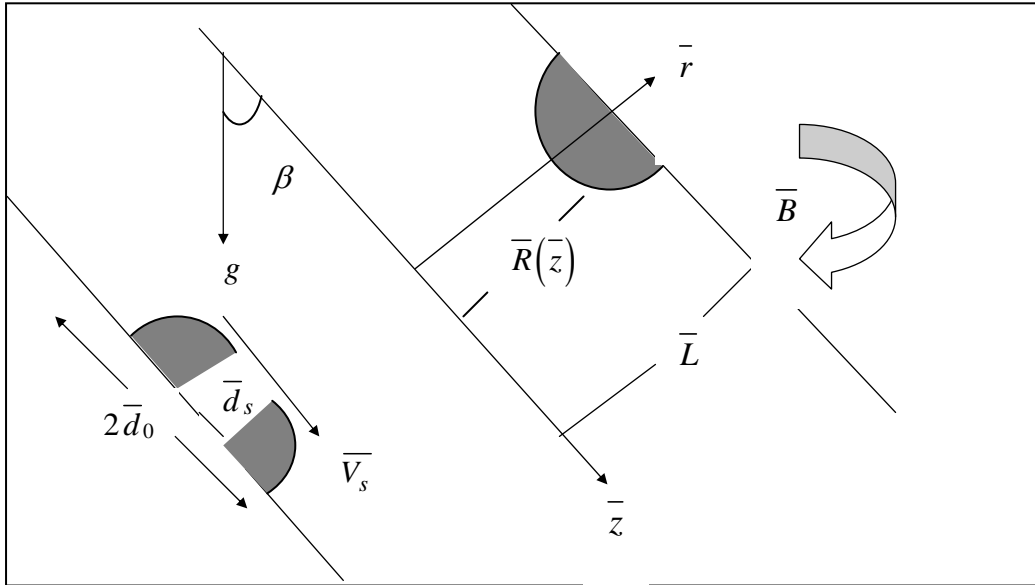
Flow configuration: Schematic figure of an inclined stenosed artery with azimuthal magnetic field

5 Conclusions

In order to elucidate the significance of our flow model and in view of the results obtained, we may conclude the following points:

1. The imposition of the magnetic field causes a decrease in each of axial velocity of blood and the wall shear stress at the stenosed section. This shows that the applied azimuthal magnetic has considerable scope in the field of treating cardiovascular diseases resulting from stenosis. The use of an azimuthal magnetic field can aid in effectively controlling the blood velocity and minimizing the large shear stress on the stenosed arterial wall.

2. The application of the slip velocity at the stenosed section leads to a growth in the axial velocity of blood. Thus, the blood flow rate in the

stenosed section may be enhanced by the imposition of slip velocity. But, the wall shear stress decreases with the imposition of the slip velocity. Hence, slip inducing medical drugs may be beneficial in effectively controlling the wall shear stress in a stenosed artery.

3. As the angle of inclination increases, the blood velocity and the wall shear stress decreases.

4. A growth in the permeability of the medium causes each of axial blood velocity and the wall shear stress to increase.

    In certain pathological conditions, the distribution of fatty cholesterol and artery-clogging blood clots in the lumen of the coronary artery may be represented by a fictitious porous medium. Therefore, an augmentation in the permeability of such porous media can enhance the blood flow rate in a stenosed artery. This may be achieved through the development of proper medical procedures and by developing medical drugs that enhance the permeability in a stenosed / clogged artery.

5. It is clear that the blood flow rate in stenosed arteries may be enhanced by imposing velocity slip at the stenosed regions and by increasing the porosity in the arteries. Thus, medical drugs that induce velocity slip at the stenosed walls and drugs that enhance the porosity in the arteries are efficient in the treatment of heart diseases induced by arterial stenosis.

6. The azimuthal magnetic field may prove to be effective in regulating the volumetric flow rate of blood in stenosed arteries.

7. An augmentation in the ratio of amplitude of body acceleration to the mean pressure causes decay in the axial velocity. However, the axial velocity registers a growth as the ratio of gravitational body force to the steady state pressure increases.

8. A rise in the ratio of amplitude of body acceleration to the mean pressure leads to a growth in the volumetric flux for small values of time and causes a fall in the volumetric flux for larger values of time. This takes place

within one full time cycle from 0 to 2π. Thus, the above behavior is attributable to the periodic natures of the body acceleration and the pulsatile pressure gradient.

9. Within one full time cycle from 0 to 2π, an increase in the ratio of gravitational body force to the steady state pressure causes the volumetric flux rate to rise.

10. Within one full time cycle from 0 to 2π, a rise in the ratio of amplitude of body acceleration to the mean pressure leads to a fall in the effective viscosity for small time and causes the effective viscosity to increase for large time. Clearly, it is a consequence of the periodic natures of the body acceleration and the pulsatile pressure gradient.

11. The effective viscosity registers a fall as the ratio of gravitational body force to the steady state pressure increases.

12. For one complete time cycle from 0 to 2π, the shear stress increases for small time and then again decreases for large time, as the ratio of amplitude of body acceleration to the mean pressure increases. Evidently, this effect is brought about by the periodic natures of the body acceleration and the pulsatile pressure gradient.

13. The shear stress exhibits a growth as the ratio of gravitational body force to the steady state pressure rises. This also indicates that an increase in the density of blood may lead to a rise in the arterial wall shear stress.

14. It follows from the preceding conclusion that the arterial wall shear stress (i.e. the so called high "blood pressure") may be minimized (i.e. effectively controlled) by lowering the density of blood in the body. This calls for the development of suitable medical procedures and drugs to achieve the same.

References:

[1]   Y. C. Fung, *Biodynamics Circulation*, Springer-Verlag, New York, 1984.

[2]   D. A. McDonald, *Blood Flow in Arteries*, Arnold, London, 1960.

[3]   M. Zamir, *The Physics of Coronary Blood Flow*, Springer, New York, 2005.

[4]   M. W. David, P. M. Christos, R. H. Stephen and N. Ku. David, "A mechanistic model of acute platelet accumulation in thrombogenic stenoses", *Annals of Biomedical Engineering*, vol. **29** (4), (2001), 321-329.

[5]   D. F. Young, "Fluid Mechanics of Arterial Stenoses", *Journal of Biomechanical Engineering*, vol. **101**, (1979), 157-175.

[6]   Z. R. Liu, G. Xu, Y. Chen, Z. Z. Teng and K. R. Qin, "An Analysis Model of Pulsatile Blood Flow in Arteries", *Applied Mathematics and Mechanics*, vol. **24**, (2003), 230-240.

[7]   L. Yao and D. Z. Li, "Pressure and Pressure Gradient in an Axisymmetric Rigid Vessel with Stenosis", *Applied Mathematics and Mechanics*, vol. **27**, (2006), 347-351.

[8]   Kh. S. Mekheimer and M. A. El Kot, "Influence of Magnetic Field and Hall Currents on Blood Flow through a Stenotic Artery", *Applied Mathematics and Mechanics*, vol. **29**, (2008), 1093-1104.

[9]   V. K. Sud and G. S. Sekhon, "Blood flow subject to a single cycle of body acceleration", *Bulletin of Mathematical Biology*, vol. **46**, (1984), 937-949.

[10] M. El-Shahed, "Pulsatile flow of blood through a stenosed porous medium under periodic body acceleration", *Appl. Math. Comput.*, vol. **138**, (2003), 479-488.

[11] E. F. Elshehawey, E. M. E. Elbarbary, M. E. Elsayed, N. A. S. Afifi and M. El-Shahed, "Pulsatile flow of blood through a porous medium under periodic body acceleration", *Int. J. Theoretical Phys.*, vol. **39** (1), (2000), 183-188.

[12] P. Brunn, "The Velocity Slip of Polar Fluids", *Rheol. Acta.*, vol. **14**, (1975), 1039-1054.

[13] A. L. Jones, "On the Flow of Blood in a Tube", *Biorheology*, vol. **3**, (1966), 183-188.

[14] L. Bennet, "Red Cell Slip at a Wall", *in vitro. Science*, vol. **155**, (1967), 1554-1556.

[15] G. Bugliarello and J. W. Hayden, "High Speed Micro Cinematographic Studies of Blood Flow", *in vitro. Science*, vol. **138**, (1962), 981-983.

[16] G. Astarita and G. Marrucci, *Principles of Non-Newtonian Fluid Mechanics*, McGraw-Hill, New York, USA, 1974.

[17] D. C. H. Cheng, "The Determination of Wall Slip Velocity in the Laminar Gravity Flow of Non-Newtonian Fluids along Plane Surfaces", *Ind. Eng. Chem. Fundamen.*, vol. **13**, (1974), 394-395.

[18] A. Kolin, "An Electromagnetic Flowmeter: Principle of Method and Its Application to Blood Flow Acceleration", *Experimental Biology and Medicine*, vol. **35**, (1936), 53-56.

[19] E. M. Korchevskii and L. S. Marochnik, "Magneto Hydrodynamic Version of Movement of Blood", *Biophysics*, vol. **10**, (1965), 411-413.

[20] M. F. Barnothy, *Biological Effects of Magnetic Fields*, Plenum Press, New York, 1964.

[21] Z. L. Xu, JMu, J. Liu, M. M. Kamocka, X. Liu, D. Z. Chen, E. D. Rosen and M. S. Alber, "Multiscale model of venous thrombus formation with surface-mediated control of blood coagulation cascade", *Biophysical Journal*, vol. **98**, (2010), 1723-1732.

[22] Z. L. Xu, N. Chen, M. M. Kamocka, E. D. Rosen and M. S. Alber, "Multiscale Model of Thrombus Development", *Journal of the Royal Society Interface*, vol. **4** (24), (2008), 705-723.

[23] Z. L. Xu, N. Chen, S. Shadden, J. E. Marsden, M. M. Kamocka, E. D. Rosen and M. S. Alber, "Study of blood flow impact on growth of thrombi using a multiscale model", *Soft Matter*, vol. **5**, (2009), 769-779.

[24] J. T. Ottesen, M. S. Olufsen and J. K. Larsen, "Applied Mathematical Models in Human Physiology", *SIAM monographs on mathematical modeling and computation*, (2004).

[25] P. Nagarani and G. Sarojamma, "Effect of body acceleration on pulsatile flow of Casson fluid through a mild stenosed artery", *Korea-Australia Rheology Journal*, vol. **20**, (2008), 189-196.

[26] E. F. EL Shehawey and W. E. L. Sebaei, "Peristaltic transport in a cylindrical tube through a porous medium", *International Journal of Mathematics and Mathematical Sciences*, vol. **24**, (2000), 217-230.

[27] E.E. Tzirtzilakis, "A Mathematical Model for Blood Flow in Magnetic Field", *Physics of Fluids*, vol. **17**, (2005), 1-15.

[28] C. J. Pennington and S. C. Cowin, "The Effective Viscosity of Polar Fluids", *Trans. Soc. Rheol*., vol.**14**, (1970), 219-238.

[29] N. Ahmed, D. P. Barua and D. J. Bhattacharyya, "MHD Pulsatile Slip Flow Of Blood Through Porous Medium In An Inclined Stenosed Artery In Presence Of Body Acceleration ", *Journal of Applied Mathematics and Bioinformatics,* vol. 4, no. 3, (2014), 1-28.